 DOI: 10.1002/maco.201307319

Non-isothermal and isothermal oxidation behaviors of AlON translucent ceramic in air

J. Q. Qi*, X. M. Xie, Y. Wang, J. Wang, L. Xiao, N. Wei, D. Wu and T. C. Lu*

The oxidation behavior of AlON translucent ceramic was investigated both in non-isothermal (from room temperature to 1573 K) and isothermal (at 1373 and 1473 K) conditions. The mass gains, phase compositions and micromorphology of oxidized samples were examined by thermogravimetric analysis (TGA), X-ray diffraction (XRD), and scanning electron microscopy (SEM), respectively. The results suggest that in non-isothermal environment the oxidation reaction starts at about 1173 K for both AlON bulk sample and powder. In isothermal condition, the mass gain indicates the two-stage reaction mechanism which starts with chemical reaction, followed by diffusion controlled stage. XRD patterns suggest that AlON is thermodynamically unstable and it partly decomposes into corundum phase Al_2O_3 and AlN during the oxidation process. SEM results indicate that different micromorphology is obtained at different temperatures in the oxidation process. The estimated apparent activation energy for the diffusion rate controlled stage from isothermal experiment is about 245.2 kJ/mol.

1 Introduction

γ-Aluminum oxynitride spinel with a central composition of $Al_{23}O_{27}N_5$ is usually considered to be a pseudobinary solid solution of Al_2O_3 and AlN. Because of its cubic structure, it can be made into fully dense polycrystalline transparent ceramic with outstanding optical, mechanical, thermal, dielectric properties, and good resistance to chemical corrosion [1,2]. Its application includes window materials, transparent armor and dome materials, high temperature lens, etc. [1,3,4]. Similar to other nitrogen ceramics, when AlON is used in high temperature environments, it is easily oxidized and its optical and mechanical properties will be substantially decreased, which tremendously limits its application. Therefore, investigation of oxidation behavior is very important for applications of AlON.

Different previous works focus on various phases of AlON [5–8]. *Corbin* and *McCauley* [5] carried out the oxidation experiment of γ-phase AlON ceramic in air and found the formation of a protective layer in oxidation process when the temperature reaches 1473 K. Beyond 1473 K, the protective layer cracked and formed fractures resulting in continuous mass gain as temperature increased. *Lefort* et al. [6] found that the AlON sample was hardly oxidized below 1473 K, above which oxidation happened continuously until 1813 K was reached. Maximum mass gain was also observed accordingly. *Wang* et al. [7] investigated the oxidation behavior of AlON powder and plate separately, in which different reaction mechanisms at low and high temperature were proposed.

Oxidation process of AlON is very complicated and can be affected by many parameters including external environment

J. Q. Qi, X. M. Xie, Y. Wang, L. Xiao, N. Wei, T. C. Lu
College of Physical Science and Engineering, Sichuan University, Chengdu 610064, Sichuan (P. R. China)
E-mail: qijianqi@scu.edu.cn, lutiecheng@scu.edu.cn

J. Q. Qi, Y. Wang, L. Xiao, T. C. Lu
Key Laboratory of Radiation Physics and Technology of Ministry of Education, Sichuan University, Chengdu 610064, Sichuan (P. R. China)

X. M. Xie
Key Laboratory of High Energy Density Physics of Ministry of Education, Sichuan University, Chengdu 610064, Sichuan (P. R. China)

J. Wang
School of Science, Sichuan University of Science and Engineering, Zigong 643000, Sichuan (P. R. China)

D. Wu
Peter A. Rock Thermochemistry Laboratory and NEAT ORU, University of California Davis, One Shields Avenue, Davis, CA 95616 (USA)

T. C. Lu
International Center for Material Physics, Chinese Academy of Sciences, Shenyang 110015, Liaoning (P. R. China)

(oxidation atmosphere, oxidation temperature, and humidity) and the internal properties of the sample (chemical and/or phase composition, grain size, pore size, pore morphology, and impurity/additive). Due to the complexity of AlON oxidation system, previous reports appear to be not consistent (see Table 1) [5–7].

In the present work, we investigated the oxidation behavior of homemade AlON translucent ceramic in both isothermal and non-isothermal conditions in air. The non-isothermal was performed up to 1573 K and the isothermal experiments were carried out at two moderate temperatures (1373 and 1473 K), at which the oxidation behavior of AlON is different from what has been reported in other literatures [5–7]. The mass gain, phase composition and micromorphology of oxidized samples were investigated and several major oxidation kinetics parameters were analyzed based on results of isothermal experiments.

2 Experimental procedure

γ-Al_2O_3 powder (~20 nm, >99.99% purity, Luming nanomaterials Co., Ltd., Liaoning, China) and aluminum powder (~2 μm, >99.9% purity, Yuanyang Aluminum Industry Co., Ltd., Henan, China) were used as raw materials to prepare AlON powder by calcining the mixtures with the certain ratio at 1973 K for 3 h [9]. The obtained AlON powder was then ground, combined with 0.1 wt% Y_2O_3 as sintering additive and molded at 20 MPa to a pellet (Φ 50 mm × 5 mm). After cold isostatic pressing at 200 MPa, the pellet was placed in a graphite resistance furnace

Table 1. The oxidation behaviors of AlON ceramics investigated by different researchers

Sample	Composition	Grain size, pore size and porosity	Oxidation mode and atmosphere	Oxidation process and results	Reference
Translucent AlON ceramic	$Al_{23}O_{27}N_5$, spinel phase	Grain size 25–100 μm, no data on the pore size, porosity <2%	Combined isothermal and non-isothermal oxidation in air	A protective oxide layer forms at temperatures less than 1473 K, and beyond this temperature, the oxide layer cracks and complete oxidation occurs resulting in the final product α-Al_2O_3	[5]
Translucent AlON ceramic	Spinel phase	Grain size 200–300 μm, no data on the pore size and density	Non-isothermal in air	The sample is hardly oxidized below 1473 K. Then oxidation can occur above this temperature and the maximum mass gain happens at 1823 K	[6]
Opaque AlON sample	$Al_{23}O_{27}N_5$ with trace of AlN	No data on the grain size and pore size, density 3.63 g/cm^3, 97.8% of the theoretical density	Isothermal oxidation in a 0.6 L/min flowing air	Oxidation begins at 1273 K. The oxidation rate is controlled by chemical reaction first until the product layer is more than 50 μm. Then the diffusion step determines the rate of the oxidation with activation energy 227 kJ/mol	[7]
Translucent AlON ceramic	$Al_{23}O_{27}N_5$ with 0.05 wt% Y_2O_3 and 0.01 wt% SiO_2	Grain size 150–200 μm, pore size 1–2 μm, density 99.1% of the theoretical density	Isothermal in static air and non-isothermal in a 40 mL flowing air	Oxidation starts at 1173 K. The oxidation also contains chemical reaction rate and diffusion rate controlled stage and the apparent activation energy for the diffusion rate controlled stage is about 245.2 kJ/mol. AlN can be observed from static air oxidation process as the instability of AlON and low oxygen pressure	This work

(Model ZT-40-20Y, Shanghai Chenxin Electric Furnace Co., Ltd., Shanghai, China) and sintered at 2153 K in N_2 flow for 15 h. Then the sample was sliced into specimens of 3 mm × 4 mm × 10 mm and polished for subsequent oxidation treatment.

The non-isothermal oxidation of AlON specimens was performed under dry air flow on a thermo-gravimeter (Model TG/STA449C, Netzsch, Germany) with a flow rate of 40 mL/min. The sample was heated from room temperature to 1573 K with a heating rate of 10 K/min. In the isothermal oxidation treatment, the ceramic specimens were heated and maintained at a desired temperature in static air atmosphere in a muffle furnace (Model 4-13, Beijing Zhongxingweiye Instrument Co., Ltd., Beijing, China). Humidity of the experimental environment was about 75%.

The mass change (Δm) of samples during isothermal oxidation was measured by an analytical balance with a sensitivity of 0.1 mg (Model ALC-110.4, Sartorius, Germany). The phase compositions of the samples were examined by X-ray diffraction (XRD, Model Dx-2500, Dandong Fangyuan Instrument Co., Ltd., Dandong, Liaoning, China) and the surface morphology of the oxidized samples was investigated by scanning electron microscopy (SEM, Model S-4800, Hitachi, Japan). The N and O content in the sample was measured by inert gas fusion (Model TC-436, Leco, USA). Potential impurity of the sample was determined by inductively coupled plasma (ICP).

3 Results and discussions

3.1 Original sample characterization

The photograph and XRD patterns of obtained sample are shown in Fig. 1. The words under the sample can be seen clearly for sample with 5 mm thickness. On the other hand, transparency inhomogeneity of the sample also can be observed, which affects the transparency significantly and results in sample translucent (in-line transmittance is merely about 30% in mid-infrared range from FTIR analysis). The XRD patterns (see Fig. 1) present all peaks from single-phase spinel aluminum oxynitride (PDF No. 48-0686: Al_5O_6N), indicating that no phase transition happened during the sintering process. The chemical analysis by inert gas method shows that the composition of AlON is around $Al_{23}O_{27}N_5$ ($9Al_2O_3 \cdot 5AlN$). From ICP method we can see that there is trace amount of Y_2O_3 (about 0.05 wt%) and SiO_2 (about 0.01 wt%) from the sample.

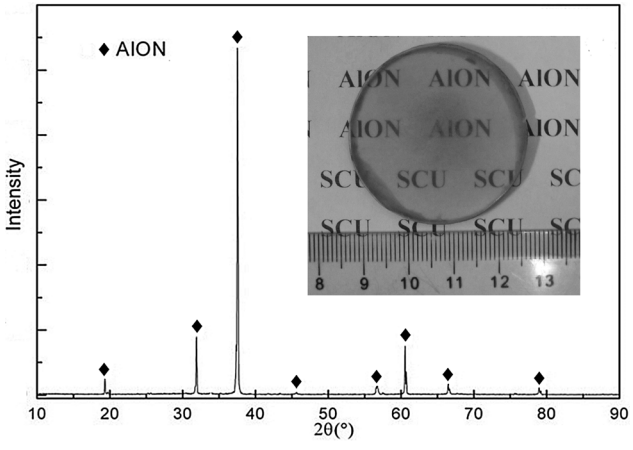

Figure 1. Photograph and XRD patterns of translucent AlON sample

3.2 Oxidation process

Based on the composition of AlON ($Al_{23}O_{27}N_5$), the oxidation reaction can be represented as,

$$Al_{23}O_{27}N_5 + 3.75O_2 \rightarrow 11.5Al_2O_3 + 2.5N_2(g) \quad (1)$$

and the final oxidation product of AlON is Al_2O_3.

Oxidation of AlON is usually a complex process involving multiple steps and different reaction mechanisms. According to *Willems's* work [10], AlON is thermodynamically stable only when the treatment temperature is higher than a certain value, which is between 1873 and 1923 K. So potential decomposition reaction that may occur in our experimental system may be represented as,

$$Al_{23}O_{27}N_5 \rightarrow 9Al_2O_3 + 5AlN \quad (2)$$

$$2AlN + \frac{3}{2}O_2 \rightarrow Al_2O_3 + N_2 \quad (3)$$

$$\Delta G_{r1} = -2\,860\,898 + 371.2T + RT\ln\left[\frac{(P_{N_2}/P_0)^{2.5}}{(P_{O_2}/P_0)^{3.75}}\right] \quad (4)$$

$$\Delta G_{r2} = -311\,183 + 167.05T \quad (5)$$

$$\Delta G_{r3} = -1\,029\,946 + 90.44T + RT\ln\left[\frac{P_{N_2}/P_0}{(P_{O_2}/P_0)^{1.5}}\right] \quad (6)$$

Hence, the change of standard Gibbs free energies of reactions (1), (2), and (3) at 1373 and 1473 K can be calculated from Equations (4–6) [11,12]. Since the calculated Gibbs free energies of reactions are all negative, these reaction processes are all thermodynamically preferable.

As previously mentioned, the oxidation of bulk AlON with O_2 is a gas–solid reaction process [7,13,14], which contains five consecutive steps [7,13]: (1) oxygen transfers from gas flow to the sample surface forming a gas–solid boundary layer, (2) oxygen transfers from surface to interface by diffusion through the layer formed in step 1, (3) oxygen reacts with AlON or decomposed AlN producing Al_2O_3 and nitrogen, (4) nitrogen diffuses from interface to sample surface, (5) nitrogen transfers from surface of AlON through gas–solid boundary layer to the gas flow.

When the fifth step is done, the oxidation of sample will repeat from the first step, until further oxidation is not possible for the deep layer. Mass, phase compositions and micromorphology will evolve accordingly.

3.3 Non-isothermal oxidation

Thermogravimetric analysis traces are shown in Fig. 2, in which the percentage of mass change $\Delta m/m_0$ is plotted as a function of temperature (Δm is the mass change and m_0 is the initial mass of the sample). The mass gain starts at about 1173 K for both bulk sample and powder, below which AlON is thermodynamically stable in atmosphere. Due to a much higher surface area which benefits oxidation process, the mass gain of powder is much more than that of bulk sample. Results from present work are consistent with observations of *Corbin* and *McCauley* [5] and *Wang* et al. [7], in which they found the oxidation of AlON bulk was initiated at 1373 and 1273 K, respectively. However, our starting temperature of oxidation is different from what was observed by *Lefort* et al. [6], which was higher than 1473 K.

3.4 Isothermal oxidation

In order to further explore the trends and oxidation behavior of AlON sample, two isothermal oxidation experiments were performed at different temperatures, 1373 and 1473 K. The oxidation dynamical curves obtained were plotted together with the results from *Corbin* and *McCauley* [5] and *Wang* et al. [7] (see Fig. 3). The relative mass gain ($\Delta m/m_0$) increases as a function of oxidation time, and degree of oxidation at 1473 K is more prominent than that of 1373 K. The sample mass increases about 0.05 wt% during the first 5 h of reaction for the two temperatures, which indicates the oxidation reaction is significant at the initial stage of the experiment. Subsequently, the rate of mass gain decreases to about 0.01 wt% as the experiment evolved. Interestingly, increasing of sample mass can be noticed even after 25–30 hours' experiment. According to *Corbin* and *McCauley* [5], there would be protective layers formed after about 10 h oxidation at 1373 and 1473 K. However, in our experiments there is no sign of formation of such a protection layer.

The XRD patterns of samples oxidized at 1373 and 1473 K for 10, 20, and 30 h are presented in Fig. 4. After oxidation at 1373 K for 10 h, corundum and AlN are identified in the final product. The intensity of XRD peaks for both samples increases as longer

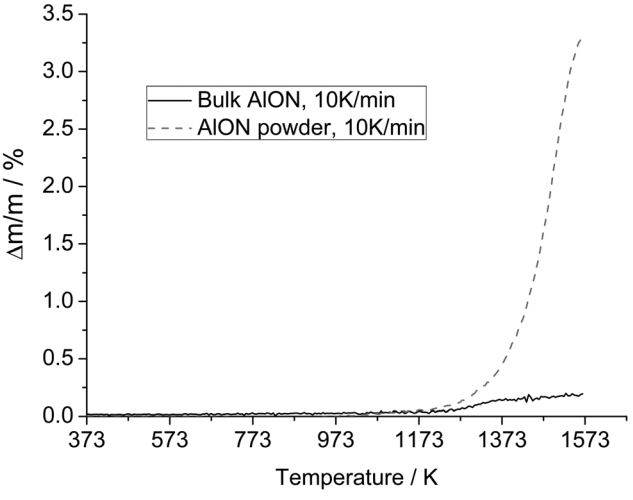

Figure 2. TGA curves of AlON bulk sample and powder in air with a heating rate of 10 K/min

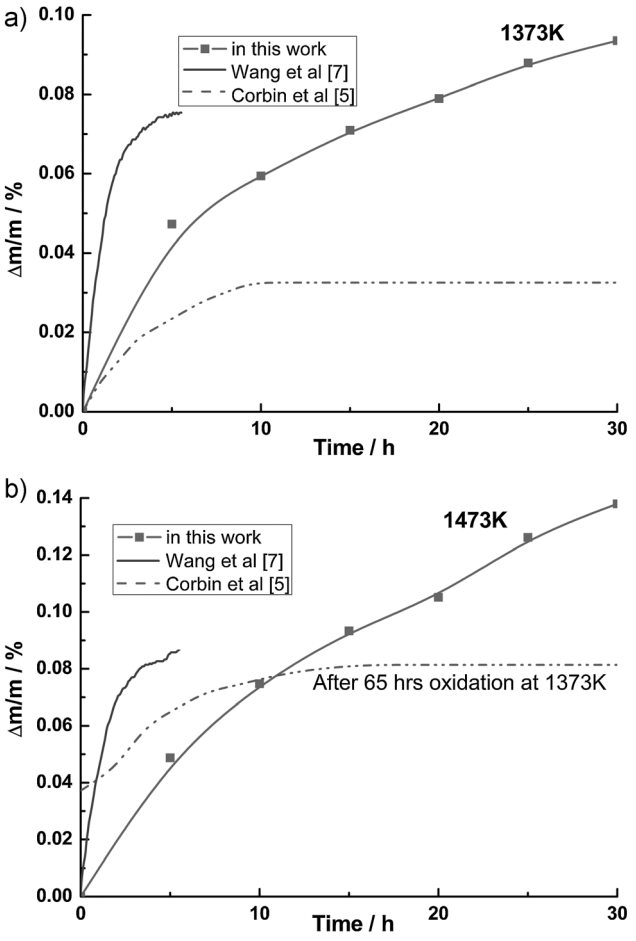

Figure 3. Oxidation dynamitic curves of bulk AlON sample oxidized at 1373 K (a) and 1473 K (b), respectively

heating time is used. However, the main phase of the sample oxidized at 1473 K for 30 h also is AlON, which is consistent with the relative mass gain which is only about 0.13% under this condition. The continued presence of AlN from the product proved that AlON is thermodynamically unstable at these two temperatures and AlN comes from the decomposition of AlON. The result is not consistent with *Wang's* results [7], from which the different phase of Al_2O_3 (such like γ-Al_2O_3) is observed and AlN is not extant in the product.

On the other hand, oxygen pressure is also a crucial factor affecting the formation of products in the oxidation process [1]. In this work, static air was used in a closed furnace so the oxygen pressure was decreasing with increasing calcination temperature. Considering the instability of AlON and the relatively low oxygen pressure, it is reasonable that AlON decomposes to Al_2O_3 and AlN in our final products.

The surfaces of samples oxidized at 1373 and 1473 K for 30 h were examined by SEM (see Fig. 5). It is clearly seen that there is significant difference between these two samples. After oxidation at 1373 K for 30 h, the whole sample surface remains flat. Tightly textured morphology is observed from the surface, which is better illustrated in the higher magnification image. Only a few little holes were observed on the surface, which suggests that "the channels" for O_2 to diffuse through is limited. However, the

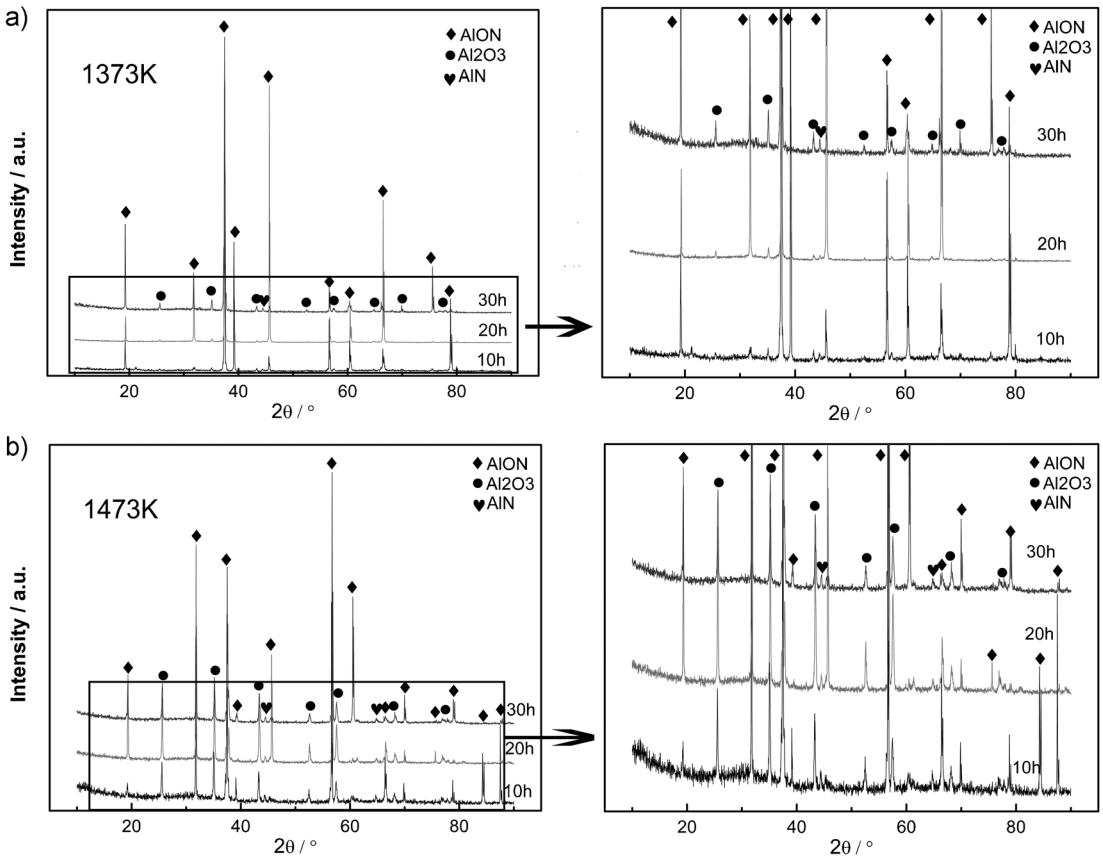

Figure 4. XRD patterns of the specimens after oxidation at 1373 K (a) and 1473 K (b) for 10, 20, and 30 h, respectively

surface oxidized at 1473 K for 30 h seems to be coarser and there are plate-like shapes formed on the surface, which enables better contact of the surface with oxygen, therefore the sample can be further oxidized easily. So surfaces with different degree of oxidation at various temperatures also correlate to their oxidation behavior.

3.5 Activation energy

In the oxidation process, $\triangle m/A$, which represents the mass gain per square centimeter, and time t have the following relation,

$$\left(\frac{\Delta m}{A}\right)^2 + B\left(\frac{\Delta m}{A}\right) = k_m t \tag{7}$$

k_m is the reaction rate constant. A and B are the parameters of mixture chemical reaction controlled rate and diffusion controlled rate, respectively. B is related to diffusion coefficient and chemical reaction constant of the surface. At the initial stage of oxidation, the surface of the sample is single phase AlON and the rate of oxidation is controlled by chemical reaction. Equation (7) can be written as,

$$\frac{\Delta m}{A} = k'_m t \tag{8}$$

In this stage, the mass increases accordingly (before 5 h in Fig. 3) and the oxidized layer is forming continuously on the sample surface.

As samples were obtained by different researchers in different ways, the internal properties such as grain size, transparency, pore size, porosity, etc. will be different. These parameters and the different oxidation temperatures will affect the oxidation rate and also will create different mass gain and product layer morphology, which accounts for the different oxidation results by different researchers. After the product layer is built, the O_2 and N_2 transportation in the oxidation process will be controlled by the diffusion and the diffusion step will determine the oxidation rate. The function (7) can be deduced as,

$$\left(\frac{\Delta m}{A}\right)^2 = k''_m t \tag{9}$$

This rate is also affected by the initial properties of the AlON sample, as different grain size, pore size, porosity, etc. from different samples will affect the diffusion rate. The reaction rates of the reaction (9) at 1373 and 1473 K can be obtained from experimental data shown in Fig. 3, and the logarithm of the rates are −14.7286 and −13.2695, respectively. The apparent activation energy E_a can be obtained based on Arrhenius equation,

$$k = k_0 \exp(-E_a/RT) \tag{10}$$

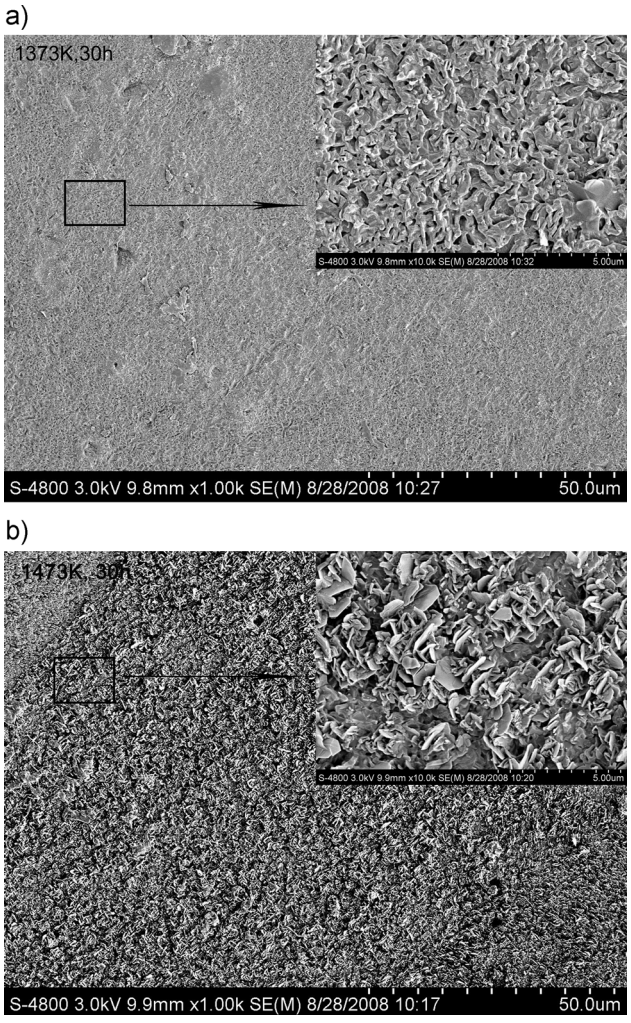

Figure 5. SEM images of oxidation surfaces of samples treated at 1373 K (a) and 1473 K (b) for 30 h

where k_0 is the frequency factor. The relationship between reaction rate constant and oxidation temperature is shown as follows,

$$k = 865.4508 \exp(-245\,213/8.31T) \quad (11)$$

The apparent activation energy for the diffusion rate controlled step from this experiment is about 245.2 kJ/mol.

4 Conclusions

The oxidation experiments of AlON specimens were performed both non-isothermally and isothermally. Major conclusions are listed below,

1. For non-isothermal oxidation, the oxidation reaction starts from 1173 K for both AlON bulk sample and powder.
2. For isothermal oxidation, the mass change as a function of oxidation time suggesting that the oxidation reaction process is initially determined by chemical reaction rate, later, driven by diffusion. Additionally, AlON is unstable in this temperature range and the phase of AlN can be observed in the products. Different micromorphology of specimens oxidized at various temperatures indicates formation of different surfaces under different thermal treatments.
3. The apparent activation energy for the diffusion rate controlled stage is about 245.2 kJ/mol in our work, which is derived from the results of isothermal oxidation. Furthermore, relationship between the reaction rate constant and oxidation temperature is concluded,

$$k = 865.4508 \exp\left(\frac{-245\,213}{8.31T}\right)$$

Acknowledgements: This work was supported by National Science Foundation of P. R. China under Grant Nos. 51002098 and 91026103, the Fund of Aeronautics Science (Grant No. 20100119003), and the Talent Introduction Program of Sichuan University of Science and Engineering (2013RC07). All analyses were done at the Analytical and Testing Center of Sichuan University.

5 References

[1] N. D. Corbin, *J. Eur. Ceram. Soc.* **1989**, *5*, 143.
[2] J. W. McCauley, N. D. Corbin, *J. Am. Ceram. Soc.* **1979**, *62*, 476.
[3] T. M. Hartnett, S. D. Bernstein, E. A. Maguire, R. W. Tustison, *Infrared Phys. Technol.* **1998**, *39*, 203.
[4] J. W. McCauley, P. Patel, M. Chen, G. Gilde, E. Strassburger, B. Paliwal, K. T. Ramesh, D. P. Dandekar, *J. Eur. Ceram. Soc.* **2009**, *29*, 223.
[5] N. D. Corbin, J. W. McCauley, *Proc. SPIE* **1982**, *297*, 19.
[6] P. Lefort, G. Ado, M. Billy, *J. Phys. Colloques* **1986**, *47*, 521.
[7] X. Wang, W. Li, D. Sichen, S. Seetharaman, *Metall. Mater. Trans. B* **2002**, *33*, 201.
[8] E. Xolin, Y. Jorand, C. Olagnon, L. Gremillard, *Corros. Sci.* **2011**, *53*, 939.
[9] J. C. Zhou, Z. J. Liao, J. Q. Qi, W. Pang, Z. M. Cheng, D. X. Wu, T. C. Lu, *Rare Metal Mater. Eng.* **2007**, *36*, 72.
[10] H. X. Willems, M. M. R. M. Hendrix, G. de With, R. Metselaar, *J. Eur. Ceram. Soc.* **1992**, *10*, 339.
[11] C. MW, JANAF, *Thermodynamic Table*, National Bureau of Standard, New York **1985**.
[12] H. X. Willems, M. M. R. M. Hendrix, R. Metselaar, G. de With, *J. Eur. Ceram. Soc.* **1992**, *10*, 327.
[13] G.-H. Zhang, X.-M. Hou, K.-C. Chou, *J. Eur. Ceram. Soc.* **2010**, *30*, 629.
[14] Z. Zhang, X. Wang, W. Li, *J. Alloys Compd.* **2005**, *387*, 74.

(Received: July 28, 2013) W7319
(Accepted: February 28, 2014)